Optical and Electrical Characterization of (PEO+Methyl Violet) Polymer Electrolytes

Subramanya Kilarkaje, V. Manjunatha, H. Devendrappa

Department of Physics, Mangalore University Mangalagangothri, Mangalore 574 199, India

Received 19 March 2010; accepted 7 April 2011
DOI 10.1002/app.34644
Published online 2 November 2011 in Wiley Online Library (wileyonlinelibrary.com).

ABSTRACT: Optical properties and electrical conductivity of polyethylene oxide (PEO) with methyl violet dopant film have studied. The complexation of the methyl violet dopant with PEO was confirmed by X-ray diffraction (XRD) and Fourier transform infrared (FTIR) spectroscopic studies. The microstructure morphology have been analyzed by scanning electron microscope (SEM) for pure and dopant films. The UV-absorption studies were made in the wavelength range 190–1100 nm for pure and doped films. The dc electrical conductivity data was collected using two probe technique in the temperature range 303–333 K. The UV–visible spectra showed the absorption band at 190 nm for pure PEO and doped from 208–224 nm region with different absorption intensities. The absorption edge, direct and indirect band gap were estimated using Mott and Davis Model. The optical activation energy can be determined using the Urbach rule, for pure PEO it was found 2.38 eV and 1.28–4.08 eV for doped films. The absorption band was shifted toward the higher frequency, the direct and indirect band gap decreases with increasing of dopant concentration, corresponds to the allowed inter band transition of electron. The dc electrical conductivity results shows that it increases with increasing dopant weight percentage and temperature which corresponds to the enhancement of charge mobility in these dye doped polymers. © 2011 Wiley Periodicals, Inc. J Appl Polym Sci 124: 2558–2566, 2012

Key words: polyelectrolyte; XRD; FTIR; SEM; optical constants; electrical conductivity and activation energy

INTRODUCTION

In recent years, the optical properties and electrical conductivity of dye doped polymers have attracted much attention in view of important applications in the optical devices with remarkable reflection, antireflection, interference, and polarization properties.[1–5] The optical and electrical properties of polymers can be suitable modified by addition of dopant depending on its complexation and reactivity with the host matrix.[6] Methyl violet doped polymers have attracted the attention due to their major applications in display device, photo resists, solar cells, ink, highlighters, lithium battery, petroleum products, leak detection method, decoder system, packing materials, wound dressing materials, antitumor agent, determination of nucleic acids.[7,8] The methyl violet has maximum absorption wavelength at 585 nm and the molecule which can accept a pair of electrons from a molecule with a free pair of associated constituent/dopant. Methyl violet contains methylated pararosaniline and amine group with nitrogen atoms having nonbonding, or lone, pair of electrons.[9]

Correspondence to: K. Subramanya (dehu2010@gmail.com).

Journal of Applied Polymer Science, Vol. 124, 2558–2566 (2012)

Since electrical properties of PEO-metal salt complexes were first reported by Wright 30 years ago and suggested appropriate applications range from solid-state batteries to solar cells, fuel cells, actuators, displays,[10,11] super capacitors, and gas sensors etc.[12–15] The dye doped polymer have emerged as a promising class of optical materials due to few advantages such as impact-resistance, ease fabrication, low density, and cost-effective technologies good association with other ions or species especially inorganic alkali, metallic salts etc.[16] Poly(ethylene oxide) (PEO is a well-known semicrystalline solid, having an extended helical structure with repeat units $[-CH_2-0-CH_2-]_n$, is the most intensively studied polymer and serves as a prototype for the structural features in most advanced dye doped polymer hosts. Since PEO has unique characteristics such as high solubility in water, organic solvents, low glass transition temperature, large dipole moment, quite low toxicity, and so on.[17] Our aim is to study the effect of methyl violet dopant on polyethylene oxide (PEO) for optimizing the optical and electrical properties to establish the suitable potential candidature. In this article, we report the results of optical and electrical characterization of methyl violet doped polymers films using UV–visible spectrometer in the frequency ranged 190–1100 nm and two probe technique using Keithley Electrometer (6514) at different temperatures.

EXPERIMENTAL METHODS

The preparation of films of pure and methyl violet doped PEO in various weight percentages (0.5, 1, 2, 5, 10, and 15%) using the solution-cast technique. The PEO ($M_w = 5 \times 10^6$) white powder had been procured from M/s. Shanghai Research Institute, Shanghai, China. Methyl violet 2B (dopant) (CDH Lab. M.W. 393.958 g/mol, $C_{24}H_{28}N_3Cl$, pH range, 0.1–2.0, yellow to violet) and methanol (AR, M.W.32) as a solvent. The PEO and methyl violet were dissolved in methanol (CH_3OH) and the mixture was stirred well at room temperature for 6–8 h. The stirred mixture was cast onto polypropylene dishes and allowed to evaporate slowly at room temperature. The films were then dried in a vacuum to eliminate all traces of the solvent and moisture. The X-ray diffraction (XRD) data recorded using Siemens X-ray diffractometer (Cu source AXS D5005) for 2θ values in the range of 0–60° at the scanning rate 1°per minute at room temperature. The IR studies were made by Perkin–Elmer IR Spectroscopy in KBr medium. A scanning electron microscope (SEM; JEOL Model JSM, 6390LV) was used to obtain the SEM images of the films. UV–visible data's measurement were carried out using a UV–VIS (UV 1800 ENG 240V) Shimadzu spectrophotometer in the wave-length range 190–1100 nm at room temperature. The dc electrical conductivity data were measured using two probe technique using PC based Keithley Electrometer (model 6514) in the temperature range 303–333 K. The films were made silver paste either sides of sample for good contact and thickness is 2.33 mm.

RESULTS AND DISCUSSIONS

XRD studies

X-ray diffraction method is very useful technique for the structural information of the material. Figure 1 shows the XRD pattern of pure and methyl violet-doped PEO films. The XRD result shows that the peaks at 2θ = 19.09° and 23.37° for pure PEO have been shifted toward the lower angle, i.e., 2θ = 18.91° and 23.17° for 15% dopant concentration. It is also observed the less intense peak in the doped films compared with that of pure PEO. These change of intensity and shifting of peaks are clearly noticed that the addition of methyl violet causes decreases in the degree of crystallinity it leads to increasing of amorphous nature in the dye doped polymer system. This indicates decrease in the crystalline phase with lowering of crystallite size of the dye doped polymer.[18,19] The reduction of crystallites size of the dye doped polymer is well agreement with the SEM results (i.e., 362.22 and 594.64 nm size). XRD pattern of 0.5% doped PEO obtained not significant because of experimental error, so it is difficult to identify and explain.

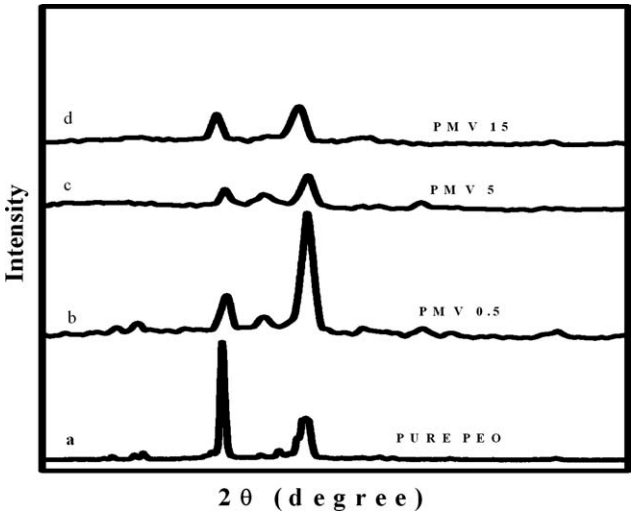

Figure 1 X-ray diffraction pattern of (a) pure PEO, (b) PMV 0.5, (c) PMV 5, and (d) PMV 15 wt % of methyl violet.

Fourier transform infrared spectroscopic spectroscopy

The FTIR is an efficient tool to study the chemical interaction and local structural change in the polymers by addition of dopant. The FTIR spectra of these materials vary according to their composition and may be able to demonstrate the occurrence of the complexation and interaction between various constituents. The FTIR spectra of pure and methyl violet doped PEO films are shown in Figure 2. The pure PEO electrolyte has distinct bands at 844 and 948 cm^{-1} which are assigned to CH_2 rocking modes in a gauche conformation, whereas bands at 1106 cm^{-1} and 1153 cm^{-1} are attributed to anti-symmetric bridge C—O—C stretching vibrations. The peaks position at 1239, 1282, 1340, and 1470 cm^{-1} are ascribed to asymmetric CH_2 twisting, symmetric CH_2 wagging and asymmetric CH_2 bending or deformation vibrations. The peak appeared at 2892 cm^{-1}, which corresponds to the —CH_2— symmetric stretching vibration and 3465 cm^{-1} are correspond to the —OH stretching.[20–25]

The O—H stretching vibration broad peak observed in between 3550–3200 cm^{-1} and it shows variation in frequency and peak intensities 3433, 3372, 3325, 3365 cm^{-1} for doped 0.5, 5, 10, and 15%, respectively, these correspond to intermolecular hydrogen bonding was established between PEO and dopant. The peak appeared in between 2950–2850 cm^{-1} are corresponds to C—H vibration stretching. The C—H stretching vibration band observed at 2892 cm^{-1} in PEO and it was split into 2932 cm^{-1}

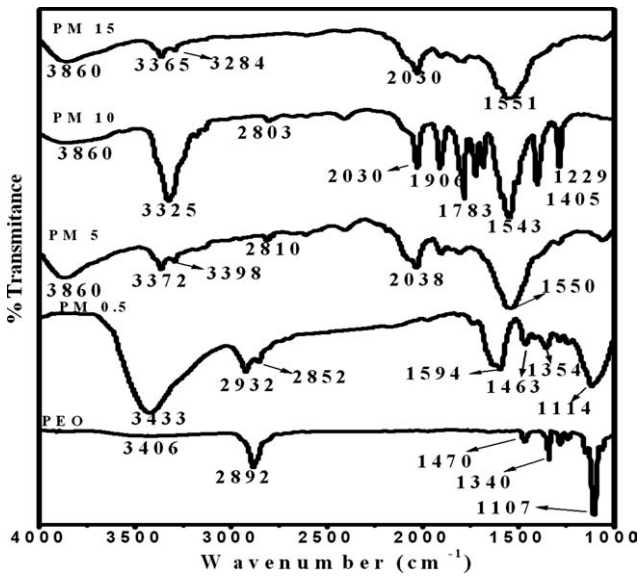

Figure 2 FTIR Spectra of Pure PEO, 0.5%, 5%, 10%, 15%, wt % of methyl violet.

and 2852 cm^{-1} for 0.5%, it decreases with increasing of dopant concentration in the polymer system. The appearance of new peak at 3860 cm^{-1} was indicating the confirmation of complexation. The peaks observed around 2000, 1680, and 1400 cm^{-1} and changes in intensity of existing peaks (and/or their disappearance) in the spectra indicates the complexation of PEO with methyl violet. The peaks appeared in between 1000–1320 cm^{-1} due to C—O stretching of ether, alcohols, carboxylic acids, and ester groups. Thus, it concluded that the oxygen of ether groups (O—CH_2) interact with dopant form complex as shown in the Scheme 1. Due to this interaction and complexation formation, the frequencies such as C—H group and C—O group will be affected as shown in the Figure 2.[26–29] The width of the C—O stretching band observed around 1107 cm^{-1} in PEO also decreases with increasing of dopant concentration and disappeared for 10 and 15% dopant.

Scanning electron microscopy

SEM micrographs of films of PEO and methyl violet doped PEO are shown in Figure 3(a–d). The surface morphology was significantly changed by the doping elements. Figure 3(a) shows rough morphology of PEO, but with 0.5 wt % of Methyl violet, a dramatic improvement of surface morphology from rough to smooth is found [Fig. 3(b)]. The smooth morphology is closely related to the reduction of PEO crystallinity with dopant. On increasing concentration of dopant, streak begins to develop on the smooth surface [Fig. 3(b,d)] and found the rod like structure with a size range 362.22 and 594.64 nm as shown in the Figure 3(d). The substantial changes in the morphology of doped PEO films confirmed as methyl violet weight percentage is increased in PEO matrix.

Optical studies

Optical absorption studies on pure and methyl violet doped PEO films were carried out to determine the optical constants such as optical band gap (E_g) and the position of the fundamental band edge. The optical spectrum of pure and doped PEO was shown in the Figure 4. From the UV–vis spectra the increase in the absorption and shift in the peak can be explained due to doping of methyl violet with PEO. On keen observation of the Figure shows the absorption maximum in the range 300 nm wavelength for PM 0.5. The distribution of absorption maximum is less than others which is due to the better complexation with the alcohol content in the doped PEO. Red shift is observed for PM 5, PM 10, and PM15, the blue shift is observed with respect to the PM 2 weight percentage. It can be interpreted that the red shift is due to the presence of Corbinol group in the methyl violet doped polymers. The long conjugation length of the polymers backbones and the aggregation of polymer chains resulted in red shift in this thin film. The aggregation effect of polymer thin film

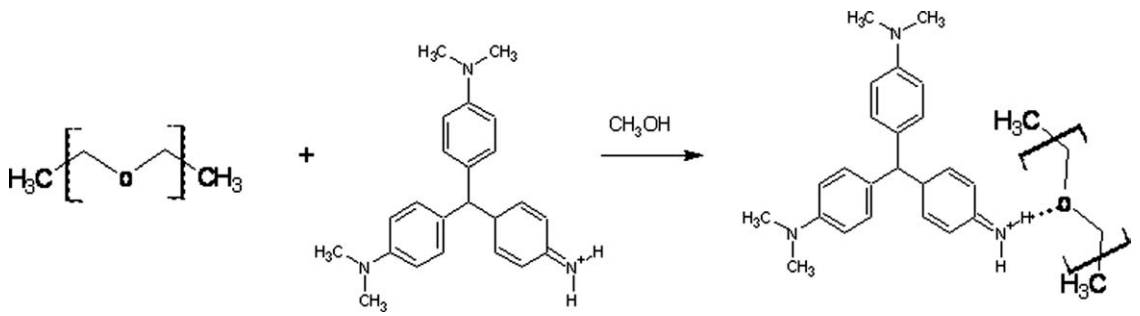

Scheme 1 Interaction between the PEO with methyl violet.

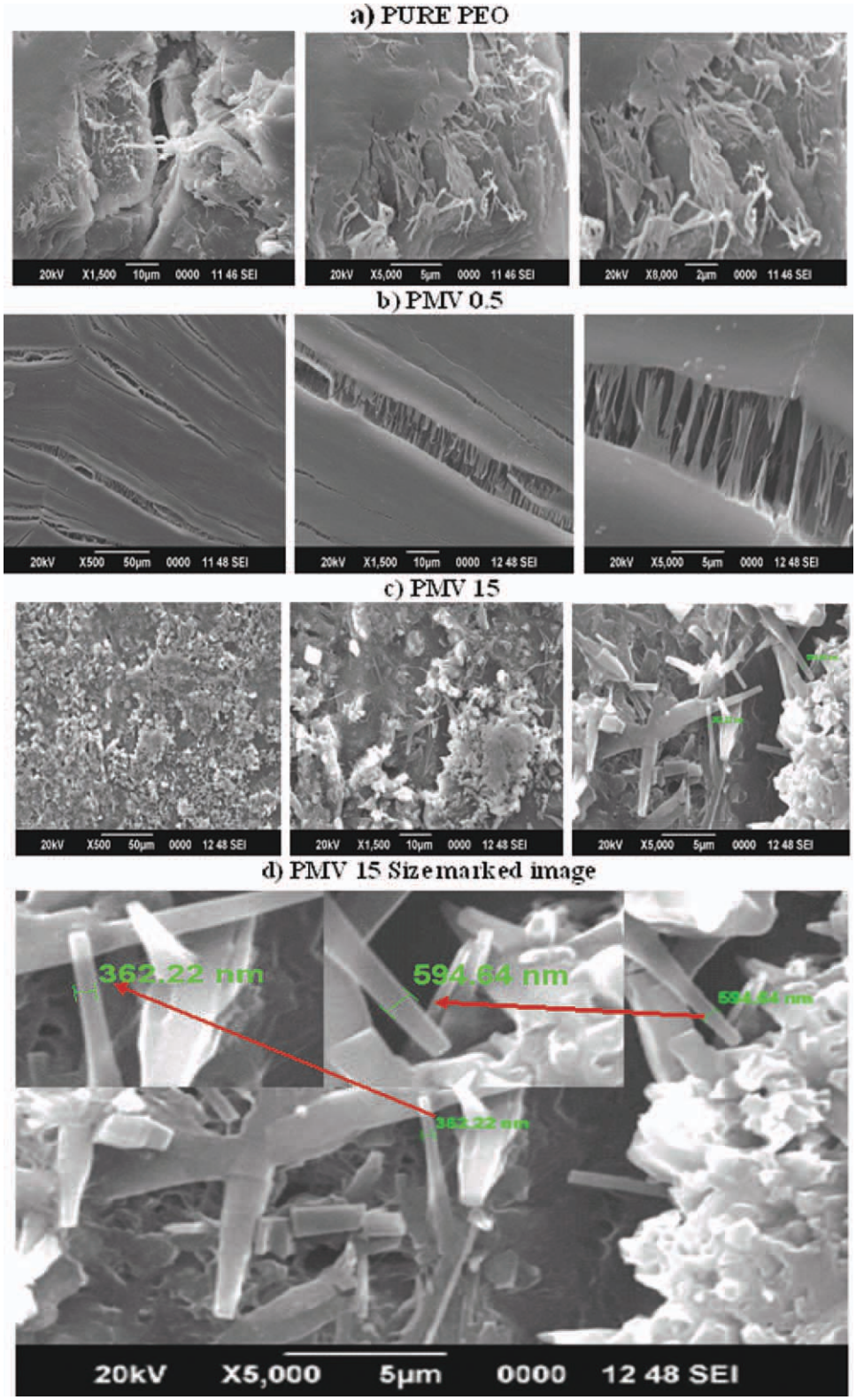

Figure 3 SEM image of the pure (a) PEO, (b) PA0.5, (c) PA15, and (d) PMV 15 size marked image [Color figure can be viewed in the online issue, which is available at wileyonlinelibrary.com.].

narrowed the energy band gap and caused a red shift. The peak wavelength of absorption of methyl violet 2B in the solid matrix shows a blue shift with respect to PM 2. This may be attributed to the decrease in the particle size. The broad absorption band is observed in the range from about 13,698–25,000 cm^{-1} is due to the presence of dye pigments, dimethyl aniline.

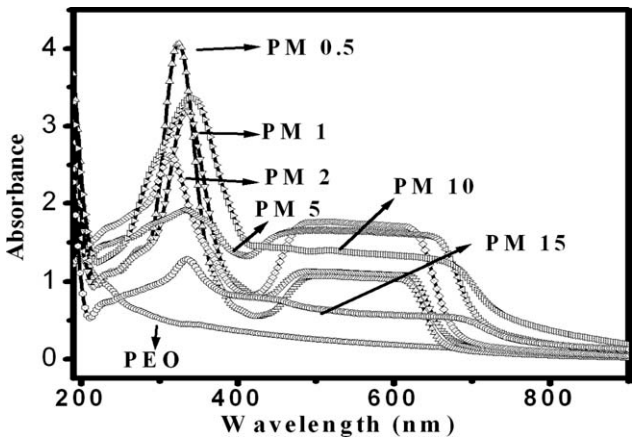

Figure 4 Plot of absorbance versus wavelength of (a) Pure PEO, (b) 0.5, (c) 1, (d) 2, (e) 5 (f) 10, and (g) 15 wt % of doped methyl violet.

The absorption coefficient was determined from the spectra using the formula,

$$\alpha = 2.303\left(\frac{A}{d}\right), \tag{1}$$

where A is absorbance and d is film thickness. The position of the absorption edge values were calculated by extrapolating the linear portions to zero absorption values of the absorption coefficient versus photon energy. It is clear from Table I that the band edge showed a decrease on doping with methyl violet up to a doping concentration and it depends upon the nature of materials.

The study of optical absorption gives information about the band structure of solids. Insulators/semiconductors are generally classified into two types: (a) direct band gap and (b) indirect band gap. In direct band gap semiconductors, the top of the valance band and the bottom of the conduction band are both laid at the same zero crystal momentum (wave vector). If the bottom of the conduction band does not correspond to zero crystal momentum, then it is called an indirect band gap semiconductor. In indirect band gap materials, transition from valence to conduction band should always be associated with a phonon of the right magnitude of crystal momentum. Davis and Shalliday[30] reported that, near the fundamental band edge, both direct and indirect transitions occur and can be observed by plotting $\alpha^{1/2}$ and α^2 as a function of energy ($h\nu$). The analysis of Thutpalli and Tomlin[31] is based on the following relations

$$(h\upsilon\,\alpha)^2 = C(h\nu - E_{\mathrm{gd}}), \tag{2}$$

$$(h\upsilon\,\alpha)^{1/2} = C(h\nu - E_{\mathrm{gi}}), \tag{3}$$

where $h\upsilon$ is the photon energy, $E_{g\mathrm{d}}$ is the direct band gap, $E_{g\mathrm{i}}$ is the indirect band gap, α is the absorption coefficient, and C is the constants. These expressions will be applied to both direct and indirect transitions helpful in the determination of the band structure of materials.[32]

When the direct gap exists, the absorption coefficient has the following dependence on the energy of the incident photon, given by Mott and Davis Model[33]

$$\alpha h\upsilon = C(h\upsilon - E_{\mathrm{g}})^{1/2}, \tag{4}$$

where E_g is the band gap, C ($C = 4\pi\sigma_o/\mathrm{nc}\Delta E$) is a constant dependent on spectrum structure, υ *is* the frequency of the incident light, and h is the Plank's constant. Thus, a plot of $(\alpha h\nu)^2$ versus photon energy ($h\upsilon$) as shown in Figure 5 should be linear. The intercept on the energy on extrapolating the linear portion of the curves to zero absorption value may be interpreted as the value of the direct band gap. For pure film the direct band gap found at 4.15 eV, while for doped polymer values are positioned between 3.38–2.24 eV are listed in the Table I.

For indirect transitions, which require photon assistance, the absorption coefficient has the following dependence on the photon energy.

$$\alpha h\upsilon = A[h\upsilon - E_{\mathrm{g}} + E_{\mathrm{p}}] + B[\mathrm{h}\upsilon - E_{\mathrm{g}} + E_{\mathrm{p}}]^{\mathbf{2}}, \tag{5}$$

where E_p is the energy of the photon associated with the transition, the A and B are constants depending on the band structure. The indirect band gaps were obtained from the plots of $(\alpha h\upsilon)^{1/2}$ versus photon energy as shown in Figure 6 and tabulated in Table I

The optical activation energy can be determined using the Urbach rule as,

$$\alpha = B_{\mathrm{exp}}(h\upsilon/E_{\mathrm{a}}), \tag{6}$$

where B is a constant and E_a is the Urbach energy, i.e., the inverse slopes of the exponential edge.

TABLE I
Absorption Edges, Optical Direct and Indirect Band Gap and Urbach Energy of Pure and Doped PEO (P = PEO & MV = Methyl Violet)

Samples	Absorption edges (eV)	Direct band gap (eV)	Indirect band gap (eV)	Urbach Energy (eV)
PEO	4.23	4.15	3.83	2.38
PMV 0.5	3.18	3.38	3.18	2.09
PMV 01	3.04	3.25	3.00	1.86
PMV 02	2.99	3.18	2.90	1.73
PMV 05	2.89	2.71	2.38	4.08
PMV 10	2.81	2.61	2.29	3.28
PMV 15	2.78	2.44	2.13	1.28

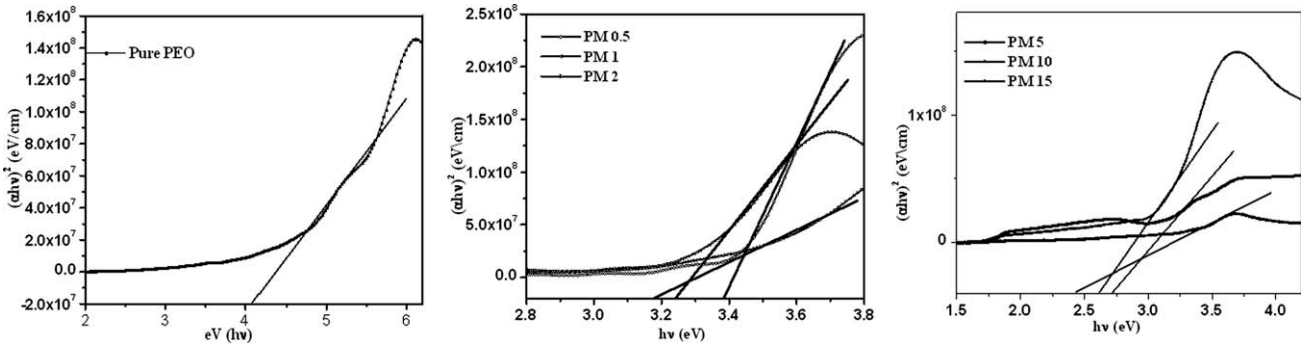

Figure 5 Direct band gap versus photon energy of (a) Pure PEO, (b) 0.5, (c) 1, (d) 2, (e) 5, (f) 10, and (g) 15 wt % of methyl violet.

The latter is interpreted as the width of the tail of localized states extending into the forbidden band gap from either the valence or conduction band.

The values of the Urbach energy Ea were determined by taking the reciprocals of the slopes of the linear portions of lnα versus photon energy (hν) plots. The values of E_a for pure PEO and doped PEO polymer complexes are listed in Table I. From results it is observed that Ea decreases with increasing weight percentage of methyl violet. The gradual decreasing values of the Urbach energy might be attributed to the formation of clusters. In case of PM5 and PM10 the Urbach energy increases may be related to the increase in the defect density due to the incorporation of dopant.

Conductivity studies

A typical conductivity plot of (PEO + methyl violet) with temperature for different weight percentage and conductivity versus weight percentage of dopant are shown in Figure 7. The conductivity of the dye doped polymer was calculated from the measured resistance (R) and the area (A) and thickness (t) of the polymer film using the formula,[34]

$$\sigma = \frac{t}{RA}. \tag{7}$$

The linear variation of conductivity with temperature suggests an Arrehenius type that may be expressed as,[35]

$$\sigma_t = \sigma_o \, e^{-\frac{E_a}{kT}}, \tag{8}$$

where σ_t is the conductivity at given temperature; where σ_0 is the pre-exponential factor, E_a the activation energy, k the Boltzmann constant, and T is the absolute temperature.

Plots of all polymer films show slightly increase in conductivity with temperature, indicating that these electrolytes exhibit an enhanced the amorphous nature.[36] The increase in conductivity with temperature can be linked to the decrease in viscosity and, hence, increased chain flexibility.[37] Since the temperature dependent conductivity data follows the Arrhenius behavior, the nature of cation transport is quite similar to that conducting polymer, where ions jump into neighboring vacant sites.[38]

In the plots (a, b, and c), it is clear that the conductivity is found to increases with increasing of temperature in pure PEO as well as in the entire doped dye

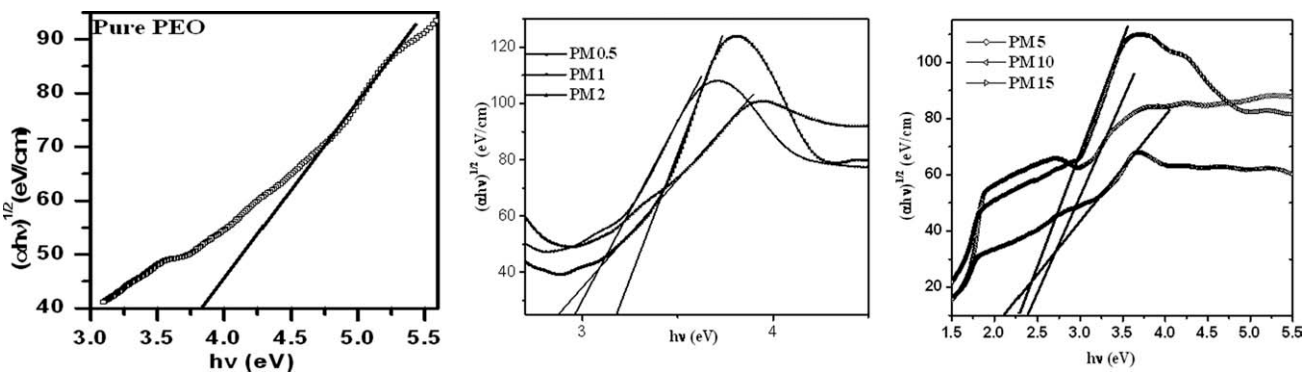

Figure 6 Indirect band gap versus photon energy of (a) Pure PEO, (b) 0.5, (c) 1, (d) 2, (e) 5, (f) 10, and (g) 15 wt % of methyl violet.

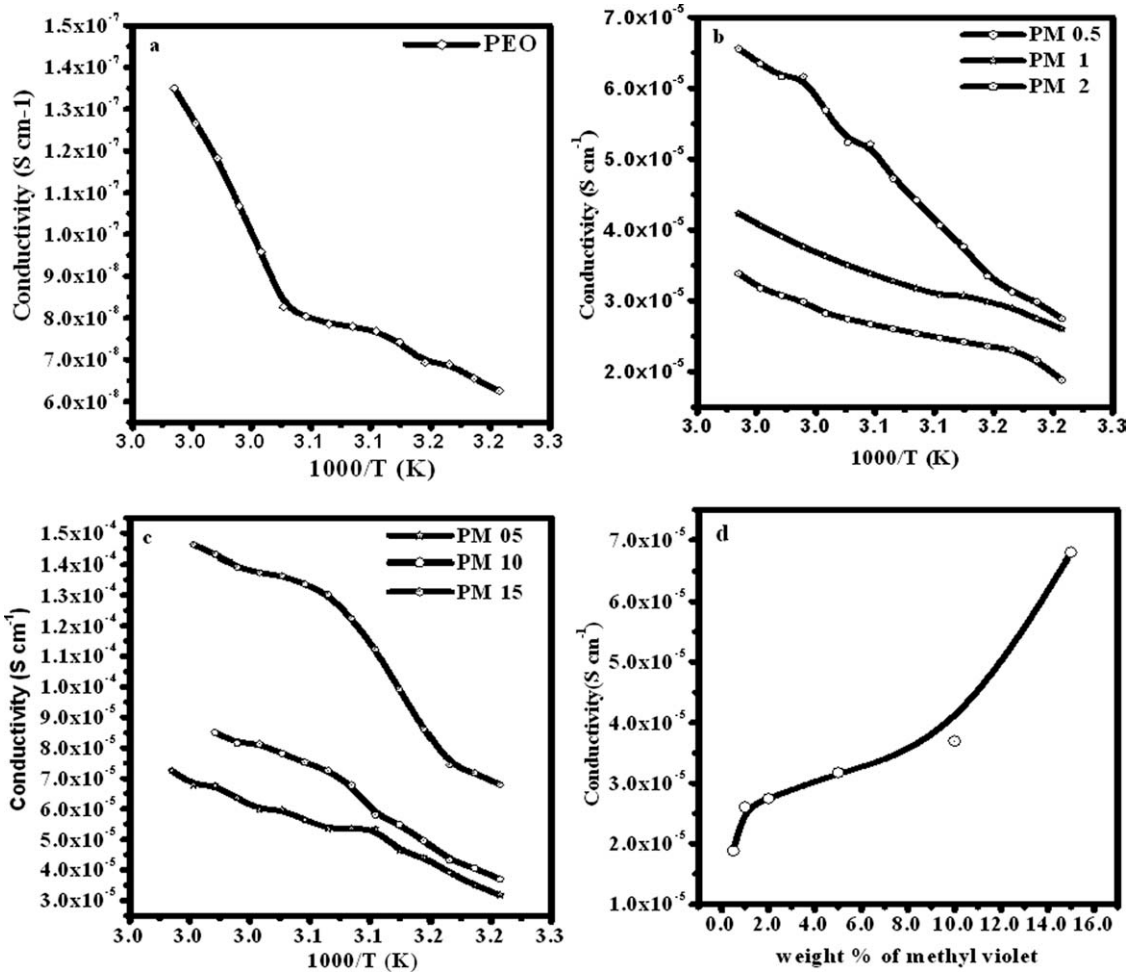

Figure 7 Electrical conductivity versus weight percentages for (a) pure PEO, (b) PMV0.5, (c) PMV1, (d) PMV 02, (e) PMV 05, (f) PMV 10, and (g) PMV 15 wt % (plot a, b, and c) and a conductivity versus weight percentage of methyl violet (plot d).

doped polymer. Similar behavior was observed in a number of PEO based electrolyte films.[39–47] The increase in the conductivity versus temperature plots may be attributed to the transitions from crystalline/semicrystalline phase to amorphous phase. We observe that its conductivity increases drastically when the temperature is raised from 303 to 333°K. The increase in the conductivity with temperature was interpreted in terms of hopping mechanism between coordination sites, local structural relaxation and segmental motion of polymer.[48] As the amorphous region increases, however the polymer chain acquires faster internal modes in which bond rotations produce segmental motion. This, in turn, favors the hopping interchain and intrachain in movements, and the conductivity of the polymer thus becomes high.[49] The electrical conductivity increases with the increasing of methyl violet concentration is also observed in the Figure 7 (plot d). The activation energies calculated from the slopes of log (σT) versus 1000/T plots, are given in the Table II.

From the Table II, it is clear that, the activation energies decreases with the increase of methyl violet concentration in all the samples. Increase in the electrical conductivity and decrease in the activation energy values of dye doped polymers can be explained on the basis that the polymer films are known to be a mixture of amorphous and crystalline region and the conductivity behavior of such films

TABLE II
Conductivity and Activation Energy (E_a) of Pure and Doped PEO

Sample	Conductivity σ in S cm^{-1} at 303 K	Activation energy E_a in eV
PEO	2×10^{-10}	0.23
PMV 0.5	2.36×10^{-8}	0.20
PMV 01	3.71×10^{-8}	0.16
PMV 02	3.30×10^{-8}	0.15
PMV 05	2.65×10^{-8}	0.28
PMV 10	9.80×10^{-8}	0.20
PMV 15	8.80×10^{-8}	0.17

may be dominated by the properties of amorphous region. Modification of the crystalline phase with increasing dopant concentration confirmed by XRD and SEM results. In case of PMV5 the activation energy was shows high because of the polymer phase is generally thought to proceed by defect assisted volume of phases rearrangements propagating along ledges at the crystal/amorphous region. The volume arrangements at the region may be of some importance and alteration in the phases of polymer system with dopant.[50] It can also interpret that the activation energies decreases due to the fact that the conductivity domain increases in number and size with the increase in weight ratios of dopant. This may facilitate the ease orientation of domains, which in turn produces paths through which ions move, leading to high conductivity.

From the results, it is noticed that both the Urbach and activation energy shows the same trend. The result reveals the variations in both the Urbach energy and the activation energy with concentration. In case of PMV5, the Urbach and activation energy occurred high because of the defects created with in the band gap region and corresponding variations are verified using Urbach energy relation or optical activation energies of doped films. The point defects are mainly resulted from the build up of the molar functional groups due to the doping.

CONCLUSIONS

We have prepared methyl violet doped PEO films using the solution-cast technique and then characterized these samples by employing the FTIR, XRD, SEM, and UV–visible spectra technique. FTIR spectra shows the significant changes in the intensities as well as frequencies it indicates that the well chemical interaction and confirmation of complexation of PEO with methyl violet. X-ray diffraction pattern reveals the increase in amorphous nature of the film with the addition of methyl violet. Scanning electron micrographs indicate gradual changes in the surface morphology of the PEO films with changes in methyl violet concentration. Optical absorption edge, optical activation energy, and optical energy gaps (both direct and indirect) showed a decreasing trend with increasing methyl violet concentration. The substantial changes of electronic absorption spectra of pure and doped PEO for direct and indirect allowed transition indicate the strong interaction between them. The electrical conductivity increases with increasing the concentration of methyl violet may due to region of alteration of phases and with temperature because of hopping mechanism. The change in conductivity can lead to the development of an excellent material that can be used as a sensor and other applications. All these results show that methyl violet dye is a promising material for application in nonlinear optical devices, electrostatic materials, and the possibility of using dye-sensitized (dye-based), photo electrochemical devices of different architecture as solar cells, and many applications that require a combination of electrical conductivity with isothermal stability.

The Authors thank the Director, USIC Karnataka University Dharwad and Sophisticated Test and Instrumentation Centre, Cochin for providing IR spectroscopy and SEM, XRD facility. Also, they thank the Mangalore University for providing the financial assistance.

References

1. Onoda, M.; Manada, Y.; Morita, S.; Yoshino, K. J Phys Soc Jpn 1989, 58, 1895.
2. Darbent, R.; Olsewska, T. Polymer 1981, 22, 1655.
3. Proneanu, S.; Torcu, R.; Brie, M.; Mihilesan, G. Mater Sci Forum 1995, 191, 241.
4. Tbata, M.; Satoh, M.; Kaneto, K.; Yoshino, K. J Phys Soc Jpn 1986, 55, 1305.
5. Bhuigan, H.; Rajapadhya, N. R.; Bhoraskar, S. V. Thin Solid Films 1988, 161, 1876.
6. Subba reddy, CH. V.; Zhu, Q.-Y.; Mai, L.-Q.; Chen, W. J Appl Electrochem 2006, 36.
7. Mukhortova, L. I. P. L.; Devyatin, A. P.; Kazakov, V. V.; Andreev, O. A. Russ RU Chem Abstr 2004, 141.
8. Marshall, C. Composite colorants containing water-soluble dyes & mineral pigments & their manufacture & use. US-117, 1992.
9. Fritz, J. S.; Bishop, E. Indicators for Non-Aqueous acid/Base Titrations in Indicators, Ed., Pergamon Press: Oxford, 1972.
10. Fenton, D. E.; Parker, J. M.; Wright, P. V. Polymer 1973, 14, 589.
11. Wright, P. V. Br Polym J 1975, 7, 319.
12. MacCallum, J. R.; Vincent, C. A. Polymer Electrolyte Review-I & II; Elsevier: London, 1987.
13. Vincent, C. A. Prog Solid State Chem 1987, 17, 145.
14. Gray, F. M. Solid Polymer Electrolytes, Fundamentals and Technological Applications; VCH: New York, 1991.
15. Conway, B. E. Electrochemical Supercapacitors: Scientific Fundamental and Technological Applications; Canada Kiuwer Academic/Plenum Publishers, New York, 1999.
16. Allcock, H. R.; Bender, J. D.; Chang, Y. Chem Mater 2003, 15, 473.
17. Pethrick, R. A.; Zaujiv, G. E. Polymer Year Book 12; Harwood Academic Publishers GMBH: Switzerland, 1995.
18. Reddy, M. J.; Chu, P. P.; Rao, U. V. S. J Power Source 2006, 158, 624.
19. Anantha, P. S.; Hariharan, K. J Solid State Ionics 2005, 176, 155.
20. Papke, B. L.; Ratner, M. A.; Shriver, D. F. Phys Chem Solids 1981, 42, 493.
21. Brandup, J.; Immergnt, E. H. Polymers-Handbook; Wiley: New York, 1966.
22. Stewart, J. E. Infrared Spectroscopy-Experimental Methods and Techniques; Marcel Dekker: New York, 1970.
23. Henniker, J. C. Infrared Spectrometry of Industrial Polymers; Academic Press: London, 1967.
24. Nakamoto, K. Infrared Spectra of Inorganic and Coordination Compounds; Wiley: New York, 1963.
25. Cross, A. D.; Jones, R. A. An Introduction to Practical Infrared Spectroscopy; Butterworths: Guildford, UK, 1969.
26. Stejskal, J.; Trchova, M.; Blinova, N. V.; Konyushenko, E. N.; Reynaud, S.; Prokes, J. Polymer 2008, 49.

27. Valentea, A.; Burrowsa, H.; Polishchukb, A.; Dominguesa, C.; Borgesc, O.; Euse'bioa, M.; Mariaa, T.; Loboa, V.; Monkmand, A. Polymer 2005, 46, 5918.
28. Al-Ahmeda A.; Mohammada, F.; Rahmanb, M.; Synth Met 2004, 144, 29.
29. Rajini, R.; Venkateswarlu, U.; Rose, C.; Sastry, T.; J Appl Polym Sci 2001, 82, 847.
30. Davis, D. S.; Shalliday, J. S. Phys Rev 1960, 118, 1020.
31. Thutupalli, G. M.; Tomlin, S. G. J Phys D Appl Phys 1976, 9, 1639.
32. Raja, V.; Mohan, V. M.; Sharma, A. K.; Narasimha Rao, V. V. R. Ionics 2009, 15, 519.
33. Mott, N. F.; Davis, E. A. Electronic Process in Non-crystalline Materials, 2nd ed.; Clarendon Press Oxford: UK, 1979.
34. Rajendran, S.; Ravi shankar Babu, K.; Renuka devi, M. Ionics 2009, 15, 61.
35. Hashmi, S. A.; Ajay kumar Maurya, K. K.; Chandra, S. Phys D Appl Phys 1990, 23, 307.
36. Michael, M. S.; Jacob, M. M. E.; Prabaharan, S. R. S.; Radha Krishna, S. Solid State Ionics 1997, 98, 167.
37. Sekhon S. S.; Pradeep K. V.; Agnihotry S. A.; Chowdari B. V. R.; Lal K.; Khare N.; Srivastava P. C.; Chandra S. Solid State Ionics; Science and Technology: Singapore, 1998.
38. Souquet, J. L.; Levy, M.; Duclot, M. Solid State Ionics, 1994, 337.
39. Madhu Mohan, V.; Raja, V.; Sharma, A. K.; Narasimha Rao, V. V. R. Mater Chem Phys 2005, 94, 177.
40. Jaipal Reddy, M.; Peter Chu, P.; Subba Rao, U. V. J Power Sources 2006, 158, 614.
41. Anantha, P. S.; Hariharan, K. J Solid State Ionics, 2005, 176, 155.
42. Wen, S. J.; Richardson, T. J.; Ghantous, D. I.; Striebel, K. A.; Ross, P. N.; Cairns, E. J. J Electroanal Chem 1996, 408, 113.
43. Papke, B. L.; Ratner, M. A.; Shriver, D. F. J Electrochem Soc 1982, 129, 1434.
44. Shin, J. H.; Kim, K. W.; Ahn, H. J.; Ahn, J. H. J Mater Sci Eng B 2002, 95, 148.
45. Armand, M. Solid State Ionics 1983, 9 &10, 745.
46. Hou, W. H.; Chen, C. Y.; Wang, C. C. J Solid State Ionics 2004, 166, 397.
47. Wang, Y.-J.; Yi, P.; Dukjoon, K. I. M. J Power Sources 2006, 159, 692.
48. Devendrappa, H.; Subba rao, U. V.; Ambika Prasad, M. V. N. J Power Sources 2006, 155, 368.
49. Narasimha Rao, V. V. R.; Mahendar, T.; Subba Rao, B. J Non-cryst Solid 1988, 104, 224.
50. Coffa, S.; Priolo, F.; Rimini, E. Crucial issues in Semiconductor Materials and Processing Technologies V-222, 1992.